Asian Journal of Chemistry; Vol. 26, No. 5 (2014), 1387-1390

ASIAN JOURNAL OF CHEMISTRY

http://dx.doi.org/10.14233/ajchem.2014.17238

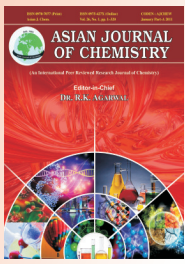

Synthesis of Mesoporous $Ce_{1-x}Sm_xO_2$ Solid Solution Materials and its Catalytic Performance†

LEI YU[1,2], FENG CHEN[1,2], JUN-CHAO QIAN[3], CHENG-BAO LIU[1,2] and ZHI-GANG CHEN[1,2,*]

[1]School of Chemistry, Biology and Materials Engineering, Suzhou University of Science and Technology, Suzhou 215009, Jiangsu, P.R. China
[2]Jiangsu Key Laboratory for Environment Function Materials, Suzhou University of Science and Technology, Suzhou 215009, Jiangsu, P.R. China
[3]School of Material Science and Engineering, Jiangsu University, Zhenjiang 212013, Jiangsu, P.R. China

*Corresponding author: E-mail: czg@mail.usts.edu.cn

Published online: 1 March 2014; AJC-14779

Novel mesoporous structural $Ce_{1-x}Sm_xO_2$ solid solution materials have been synthesized *via* a facile approach of evaporation-induced self-assembly (EISA) in the presence of nitrate as inorganic species and triblock copolymers P_{123} as template. The detailed charaterization by power X-ray diffraction, transmission electron microscope, selected electron diffraction revealed the samples possessing fluorite-structure with the average grain size of 7 nm. Furthermore, N_2 adsorption-desorption measurement illustrated the particular hierarchical porous textural $Ce_{1-x}Sm_xO_2$ solid solution with the pores size in diameter between 2 to 4 nm and the maximun surface area of 106 m^2/g. The temperature-programmed reduction of H_2 (H_2-TPR) result confirmed that the ceria-samarium solid solution owned more vacancies than pure CeO_2, hence the double level pores textural $Ce_{1-x}Sm_xO_2$ seem to be potential candidates for catalytic aspect.

Keywords: $Ce_{1-x}Sm_xO_2$, Solid solution, Mesoporous, Catalytic performance.

INTRODUCTION

Since the ordered mesoporous silica M41S series first successfully synthesized by the scientists of Mobil[1-3], the ever increasing number of researchers have devoted themselves to developing advanced meso-textured inorganic or organic-inorganic hybrid materials using various types of organic template. Because of well-defined pore structure, uniform pores size in diameter between 2 to 50 nm and large surface area, mesoporous materials were known to apply in the fields of catalysis, optics, photonics, sensors, separation, drug delivery, sorption, acoustic or electrical insulation[4-8]. However, the conventional amorphous pore wall of most mesoporous materials using surfactant template, limited their application in many fields because of the poor thermal and mechanical stability[9]. Recently, non-silica oxide mesoporous materials, such as transition metal oxides, have been investigated[4]. The transition metal oxides mesoporous materials synthesized by evaporation-induced self-assembly (EISA) method were highly crystallized and possess hierarchical ordered structure on meso-scale as well as on atom-scale[9].

Ceria belonging to an indispensable family of transition metal oxides, which is widely used in polishing agents, oxygen sensor, solid oxide fuel cells (SOFC), ceramic materials, especially catalysis[10-15]. Growing number of recent reports have been dedicated to ceria-containing solid solution or composite oxides, which could improve physical/chemical properties of the ceria-based materials, such as catalytic performance. Novel nanocrystalline $Ce_{1-x}La_xO_{2-\delta}$ ($x = 0.2$) solid solution has been successfully prepared by Benjaram, resulting that the $Ce_{1-x}La_xO_{2-\delta}$ ($x = 0.2$) solid solution exhibited better catalytic properties due to smaller crystallite size, facile reduction, profound bulk oxygen mobility and enhanced OSC[16]. Eva Díaz and cooperator researched ceria-zirconia mixed oxides as catalysts for combustion of volatile organic compounds using inverse gas chromatography[17]. However, compared to MO_X-CeO_2 (M = Cu, Mn, Fe, Co and Ni) mixed oxides, Sm^{3+} doped CeO_2 solid solution has rarely been reported and thus the unique performance of $Ce_{1-x}Sm_xO_2$ remains to be further investigated in the experimental process.

The grain size, morphology, pore shape and distribution, oxygen vacancies, which enormously determine the physico-chemical properties of materials. In the present work, we report the fabrication of the micro-mesoporous textural $Ce_{1-x}Sm_xO_2$ solid solution *via* evaporation-induced self-assembly by template, meanwhile, the catalytic performance and formation of two series of pores were also investigated.

†Presented at The 7th International Conference on Multi-functional Materials and Applications, held on 22-24 November 2013, Anhui University of Science & Technology, Huainan, Anhui Province, P.R. China

EXPERIMENTAL

In this work, 1 g of P_{123} ($EO_{20}PO_{70}EO_{20}$, Sigma-Aldrich) was dissolved into a mixed solution of 15 mL ethanol and 5 mL deionized water, then a total quantity of 0.005 mol of cerium nitrate [$Ce(NO_3)_3{\cdot}6H_2O$,SCRC] and samarium trinitrate [$Sm(NO_3)_3$, SCRC] on the basis of proportion of Sm^{3+} molar fraction ranging from 0 to 0.2 were added into above mixed solution. The mixture was magnetic stirred for 5 h to ensure homogeneous mixing before being transferred into a 100 mm in diameter petri dishes with a micropipette. Then the petri dishes were placed in an oven for 72 h at 80 ºC, after 72 h aging and dry, subsequently the gel was calcined at 400ºC for 3 h with a muffle furnace to remove the triblock copolymer P_{123}.

The powder X-ray diffraction (PXRD) patterns were observed by using a Rigaku X-ray diffractometer CuK_α radiation. The average grain size D was calculated according to Scherrer equation: $D = 0.89\lambda/\beta \cos\theta$, where θ was the diffraction angle of the main peak and β is the full width at half maximum (FWHM). TEM characterization was implemented using a JEM-2010 emission transmission electron microscope operating at an accelerating voltage of 200 kV. The N_2 adsorption-desorption measurement was carried out using Micromeritics ASAP 2010 at 77 K; the specific surface area and the pore size distribution were calculated using Brunauer-Emmett-Teller (BET) and Barrett-Joyner-Halenda (BJH) methods. Reducibility of the samples were examined by H_2-TPR , which were performed with a quartz reactor equipped with a Tianjin XQ TP5000 autoadsorption apparatus.

RESULTS AND DISCUSSION

The XRD patterns of as-synthesized products are shown in Fig. 1. It can be found in this pattern, the typical diffraction peaks at 2θ = 28.6, 33.1, 47.4, 56.3, 69.5, 76.6 show the face-centered cubic fluorite structure of ceria (JCPDS No. 34-0394) and exhibit in consistent with the fluorite cubic phase (111), (200), (220), (311), (400) and (331) diffraction planes, respectively. The XRD patterns of ceria-samarium solid solution exhibited shifts of diffraction peaks toward lower 2θ values with respect to pure ceria and can be found becoming broader and lower in intensity with increasing of Sm^{3+} components, which attribute to incorporation of doping of CeO_2 with Sm^{3+}. The ionic radius of Sm^{3+} (0.096 nm) is smaller than Ce^{4+} (0.097 nm), hence lattice contraction is expected owing to the partial substitution of Ce^{4+} with Sm^{3+}. Compared with pure ceria (5.410 Å), the cell parameter "a" of $Ce_{1-x}Sm_xO_2$ solid solution calculated using the most prominent (111) planes is decreased to about 5.391 Å and is in good agreement with above analysis (Table-1).

TABLE-1
AVERAGE CRYSTALLITE SIZE AND LATTICE PARAMETER OF SAMPLES

Sample	a	b	c
Crystallite size (nm)	7.9	7.9	7.7
Lattice parameter (Å)	5.410	5.394	5.391

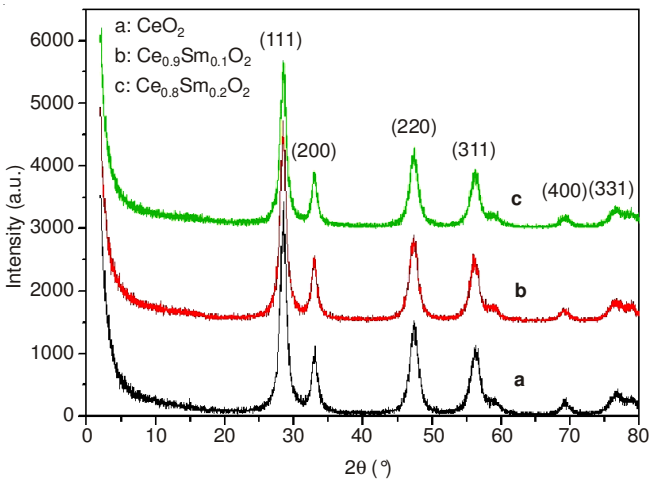

Fig. 1. Power X-ray diffraction patterns of mesoporous $Ce_{1-x}Sm_xO_2$

Transmission electron microscopic (TEM) and selected electron diffraction (SAED) analyses are undertaken to monitor the evolution of the morphology and structure and to confirm the pore size. As can be seen from the TEM images (Fig. 2a), there are the worm-like porous structure with the size of approximately 2-4 nm, which indicating that the pure CeO_2 by using P_{123} template has mesoporous structure and is made of many small crystals. Fig. 2b illustrates the TEM image of $Ce_{0.9}Sm_{0.1}O_2$ solid solution. The shape of pores is regularly hexagonal, which are consistent with six square accumulation structure gathered and formed by triblock copolymers P_{123} in the solution. The distances between the adjacent lattice fringes correspond to the interplanar distances of the cubic CeO_2(111), which is d_{111} = 0.313 nm (Fig. 2c). TEM image (Fig. 2d) of the $Ce_{0.8}Sm_{0.2}O_2$ already indicates that the material has small crystals and mesoporous structure, which was due to sintering.

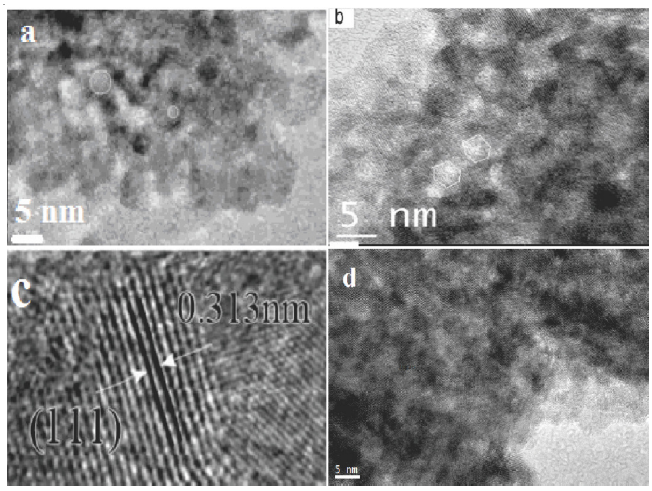

Fig. 2. TEM images of mesoporous CeO_2 (a), $Ce_{0.9}Sm_{0.1}O_2$ (b) $Ce_{0.8}Sm_{0.2}O_2$ (d) and HRTEM images of $Ce_{0.9}Sm_{0.1}O_2$ (c)

The N_2 adsorption-desorption isothrem and pore-size distribution isothern provide further information about structure of samples in Fig. 3. It shows that the curves of the N_2 adsorption-desorption isotherms for three samples are similar and intermediate between types I and IV according to the IUPAC classification[18,19].

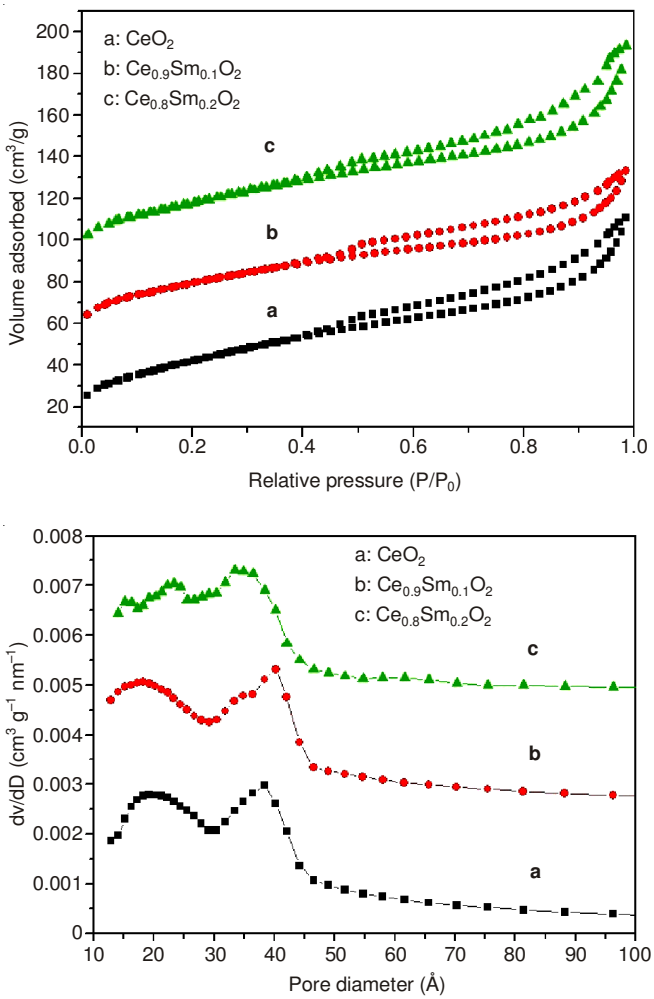

Fig. 3. N_2 adsorption-desorption isotherm and pore-size distribution plot of samples

Its shape indicates the existence of mesopores[20], which conforms the results of TEM. The surface area of samples calculated *via* Brunauer-Emment-Teller (BET) are shown in Table-2. The pore-size distribution isotherm suggested that pores size in diameter at 2 to 4 nm, respectively, belonging to the micro- and mesoporous scope. This further confirms the above information on the structure of samples.

TABLE-2
SURFACE AREA OF SAMPLES

Sample	a	b	c
S_{BET} (m^2 g^{-1})	110	93	113

The redox properties of samples are investigated by H_2-TPR experiments. Fig. 4 shows the H_2-TPR of samples synthesized by triblock copolymers as template. The TPR of pure CeO_2 indicated two reduction peaks at 450 and 760 ºC. The peak below 500 ºC is attributed to the reduction of surface oxygen and peak observed above 700 ºC is assigned to the reduction of bulk oxygen[21]. The surface oxygen has higher activity, so it can be reduced under the low temperature. Compared to surface oxygen, the bulk oxygen with low-activity needs to be reduced at a higher temperature. With the introduction of Sm^{3+}, H_2-TPR curve of $Ce_{1-x}Sm_xO_2$ (x = 0.1, 0.2) solid solution can be influenced, the low temperature

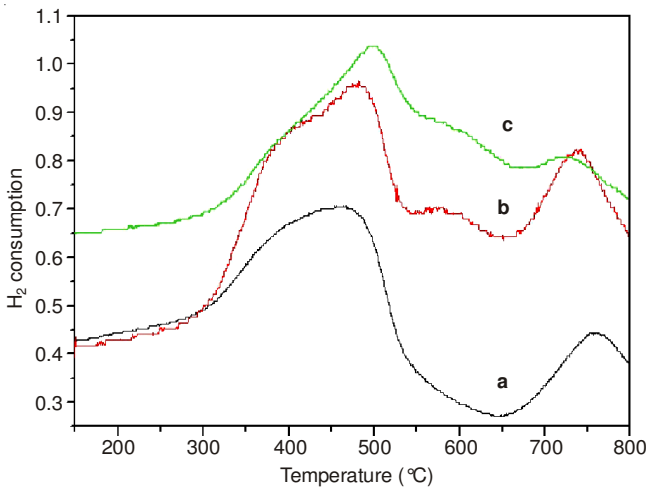

Fig. 4. H_2-TPR profiles: (a) CeO_2, (b) $Ce_{0.9}Sm_{0.1}O_2$, (c) $Ce_{0.8}Sm_{0.2}O_2$

reduction peak toward higher temperature and the high temperature reduction peak toward lower temperature. The result could be attributed to oxygen vacancy created by the partial substitution of Ce^{4+} with Sm^{3+} and the oxygen mobility enhanced *via* mesoporous structure.

Conclusion

The $Ce_{1-x}Sm_xO_2$ (x = 0, 0.1, 0.2) solid solution with mesoporous structure, large surface area and superior catalytic performance have been synthesized *via* EISA method. The $Ce_{1-x}Sm_xO_2$ (x = 0.1, 0.2) solid solution with template structure has a higher oxygen capacity at low-temperature than pure CeO_2, which attribute to its mesoporous structure. The porous structure increases the surface area, which can be proved by the N_2 adsorption and desorption. The higher surface area of $Ce_{1-x}Sm_xO_2$ provides more surface oxygen, which in agreement with results of predecessors. Moreover, the pore is conducive to mass transfer, so it is good to reducing gas (hydrogen) to the oxide surface, and by reacting to surface oxygen to promote low-temperature reduction process more effectively.

ACKNOWLEDGEMENTS

National Natural Science Foundation of China (21071107, 21277094, 21103119); Production and Research Collaborative Innovation Project of Jiangsu Province (BY2012123); Natural Science Foundation of Jiangsu Province (BK2012167); Science and Technology Pillar Program (Industry) of Jiangsu Province (BE2012101); Collegiate Natural Science Fund of Jiangsu Province (12KJA430005, 11KJB430012); A Project Funded by the Priority Academic Program Development of Jiangsu Higher Education Institutions (PAPD); Applied Basic Research Project of Suzhou (SYG201242, SYG201316); Jiangsu Key Laboratory of Material Tribology (Kjsmcx2011001); Youth project of Suzhou university of science and technology (XKQ201213).

REFERENCES

1. J.S. Beck, J.C. Vartuli, W.J. Roth, M.E. Leonowicz, C.T. Kresge, K.D. Schmitt, C.T.-W. Chu, D.H. Olson and E.W. Sheppard, *J. Am. Chem. Soc.*, **114**, 10834 (1992).
2. C.T. Kresge, M.E. Leonowicz, W.J. Roth, J.C. Vartuli and J.S. Beck, *Nature*, **359**, 710 (1992).

3. M.E. Davis, *Nature*, **417**, 813 (2002).
4. X.B. Zhao, F. Chen, J. You, X.Z. Li, X.W. Lu and Z.G. Chen, *J. Mater. Sci*., **45**, 3563 (2010).
5. X.Z. Li, C.Y. Ni, F. Chen, X. Lu and Z. Chen, *J. Solid State Chem*., **182**, 2185 (2009).
6. J. Fan, S. Boettcher and G.D. Stucky, *Chem. Mater*., **18**, 6391 (2006).
7. Y. Wan, H.F. Yang and D.Y. Zhao, *Acc. Chem. Res*., **39**, 423 (2006).
8. A.I.Y. Tok, S.W. Du, F.Y.C. Boey and W.K. Chong, *Mater. Sci. Eng. A*, **466**, 223 (2007).
9. W.H. Shen, X.P. Dong, Y.F. Zhu, H. Chen and J. Shi, *Micropor. Mesopor. Mater*., **85**, 157 (2005).
10. S. Masson, P. Holliman, M. Kalaji and P. Kluson, *Mater. Chem*., **19**, 3517 (2009).
11. J.L.M. Rupp, A. Infortuna and L. Gauckler, *Acta Mater*., **54**, 1721 (2006).
12. X. Liu, K. Zhou, L. Wang, B. Wang and Y. Li, *J. Am. Chem. Soc*., **131**, 3140 (2009).
13. Q.Q. Huang, X.M. Xue and R.X. Zhou, *J. Mol. Catal. Chem*., **331**, 130 (2010).
14. P. Borker and A.V. Salker, *Mater. Chem. Phys*., **103**, 366 (2007).
15. W. Zhang, D. Zhang, T.X. Fan, J.J. Gu, J. Ding, H. Wang, Q.X. Guo and H. Ogawa, *Chem. Mater*., **21**, 33 (2009).
16. B.M. Reddy, L. Katta and G. Thrimurthulu, *Chem. Mater*., **22**, 467 (2010).
17. E. Díaz, B. de Rivas, R. López-Fonseca, S. Ordóñez and J.I. Gutiérrez-Ortiz, *J. Chromatogr. A*, **1116**, 230 (2006).
18. H.Q. Zhu, Z.F. Qin, W.J. Shan, W.J. Shen and J.G. Wang, *Catal*, **225**, 267 (2004).
19. K.S. Sing, D.H. Everett and R.A.W. Haul, *Appl. Chem*, **57**, 603 (1985).
20. V. Perrichon, A. Laachir, S. Abouarnadasse, O. Touret and G. Blanchard, *Appl. Catal. A*, **129**, 69 (1995).
21. J.M. Zhou, L. Zhao, Q.Q. Huang, R.X. Zhou and X.K. Li, *Catal. Lett*., **127**, 277 (2009).